

4

REPORT DOCUMENTATION PAGE

AD-A221 079

DTIC  
SELECTE  
APR 30 1990  
S  
D  
GD

1. REPORT SECURITY CLASSIFICATION Unclassified		1b. RESTRICTIVE MARKINGS	
2. SECURITY CLASSIFICATION AUTHORITY DECLASSIFICATION/DOWNGRADING SCHEDULE		3. DISTRIBUTION/AVAILABILITY OF REPORT Unclassified/Unlimited	
PERFORMING ORGANIZATION REPORT NUMBER(S) ONR Technical Report #26		5. MONITORING ORGANIZATION REPORT NUMBER(S)	
4. NAME OF PERFORMING ORGANIZATION Corrosion Research Center ADDRESS (City, State, and ZIP Code) University of Minnesota Minneapolis, MN 55455		6a. OFFICE SYMBOL (If applicable)	
7a. NAME OF MONITORING ORGANIZATION Office of Naval Research, Resident Rep.		7b. ADDRESS (City, State, and ZIP Code) Federal Building, Room 286 536 South Clark Street Chicago, IL 60605-1588	
8. NAME OF FUNDING/SPONSORING ORGANIZATION Office of Naval Res. & the Def Adv Res Projects Agency		8b. OFFICE SYMBOL (If applicable) Code 1113	
9. PROCUREMENT INSTRUMENT IDENTIFICATION NUMBER Contract No. N00014-88-K-0360		10. SOURCE OF FUNDING NUMBERS	
3c. ADDRESS (City, State, and ZIP Code) 800 North Quincy Street Arlington, VA 22217-5000		PROGRAM ELEMENT NO.	PROJECT NO.
		TASK NO.	WORK UNIT ACCESSION NO.

11. TITLE (Include Security Classification)  
Quartz Crystal Microbalance Study: Ionic Motion Across Conducting Polymers

12. PERSONAL AUTHOR(S)  
Katsuhiko Naoi, Mary Lien, and William H. Smyrl

13a. TYPE OF REPORT Technical	13b. TIME COVERED FROM 1/1/89 TO 3/1/90	14. DATE OF REPORT (Year, Month, Day) March 15, 1990	15. PAGE COUNT 28
----------------------------------	--	---	----------------------

16. SUPPLEMENTARY NOTATION  
submitted to J. Electrochm. Soc.

17. COSATI CODES			18. SUBJECT TERMS (Continue on reverse if necessary and identify by block number) quartz crystal microbalance, QCM, conducting polymer, polypyrrole, redox polymer
FIELD	GROUP	SUB-GROUP	

19. ABSTRACT (Continue on reverse if necessary and identify by block number)  
In-situ monitoring of mass change was performed during electrochemical growth and redox cycling of a conducting polymer (polypyrrole) on a quartz crystal microbalance. For the polypyrrole films grown with large polymeric anions (poly(4-styrenesulfonate) and polyvinylsulfonate), mostly cations and solvent molecules were inserted and removed to compensate charge in polypyrrole. The films formed with medium sized anions (tosylate) showed both anion and cation motion during the redox process. The films prepared in the presence of small anions (ClO<sub>4</sub><sup>-</sup> and BF<sub>4</sub><sup>-</sup>) showed mostly anion motion, but cation motion also became significant for higher oxidation and/or reduction state.

20. DISTRIBUTION/AVAILABILITY OF ABSTRACT <input checked="" type="checkbox"/> UNCLASSIFIED/UNLIMITED <input type="checkbox"/> SAME AS RPT <input type="checkbox"/> DTIC USERS		21. ABSTRACT SECURITY CLASSIFICATION Unclassified	
22a. NAME OF RESPONSIBLE INDIVIDUAL Boone B. Owens		22b. TELEPHONE (Include Area Code) (612) 625-1332	22c. OFFICE SYMBOL

## QUARTZ CRYSTAL MICROBALANCE STUDY: IONIC MOTION ACROSS CONDUCTING POLYMERS

Katsuhiko Naoi\*, \*\*, Mary Lien<sup>+</sup> and William H. Smyrl\*

Corrosion Research Center,

Department of Chemical Engineering and Materials Science,

University of Minnesota, Minneapolis, Minnesota 55455, U.S.A.

Accession For	
NTIS GRA&I	<input checked="" type="checkbox"/>
DTIC TAB	<input type="checkbox"/>
Unannounced	<input type="checkbox"/>
Justification	
By	
Distribution /	
Availability Codes	
Dist	Avail. and/or Special
A-1	

### ABSTRACT

In-situ monitoring of mass change was performed during electrochemical growth and redox cycling of a conducting polymer (polypyrrole) on a quartz crystal microbalance. For the polypyrrole films grown with large polymeric anions (poly(4-styrenesulfonate) and polyvinylsulfonate), mostly cations and solvent molecules were inserted and removed to compensate charge in polypyrrole. The films formed with medium sized anions (tosylate) showed both anion and cation motion during the redox process. The films prepared in the presence of small anions ( $\text{ClO}_4^-$  and  $\text{BF}_4^-$ ) showed mostly anion motion, but cation motion also became significant for higher oxidation and/or reduction state.

### INTRODUCTION

Utilization of the quartz crystal microbalance (QCM) in conjunction with electrochemistry allows one to determine mass change on the electrode simultaneously with electrochemical reactions under in-situ conditions. The combination of mass change and

\* Electrochemical Society Active Member

+ Electrochemical Society Student Member

\*\* Present Address: Department of Applied Chem., Faculty of Engineering,  
Tokyo University of Agriculture & Technology  
Koganei, Tokyo 163, Japan

Key Words: QCM, Conducting Polymer, Capacitor, Ionic motion, Mass change

electrochemical reaction rate measurements have several advantages that have been demonstrated for the following cases: 1) electrodeposition of metals<sup>1</sup>, 2) metal dissolution(Ni)<sup>2</sup>, and 3) redox cycling of conducting polymers(polypyrrole<sup>3</sup>, polyaniline<sup>4</sup>) and redox polymers (polyvinylferrocene<sup>5</sup>). In the present study, the method was applied to monitor the mass change due to electrochemical polymerization and the subsequent redox reactions of polypyrrole. The emphasis of the paper is to survey the insertion/extraction of ions, either anions or cations or both, that are induced by subsequent redox cycling of the polymer. By incorporating anions of different size during electropolymerization, it will be shown that pyrrole can be made to show different polymerization and redox behavior. As already suggested by previous papers<sup>12,13</sup>, the charge efficiency of polymer growth depends on the kind of co-existing ions(mostly anions but also cations). The effect seems to be associated with the chemical nature(nucleophilic character) and the size of anions.

Oxidation and reduction of the grown polypyrrole films were carefully investigated, and found to be different from film to film. During the oxidation/reduction of the films, the proportion of the numbers of anions to cations in the charge compensation process was estimated and compared to the predicted mass change calculated from the charge monitored simultaneously by cyclic voltammetry. The anion/cation ratio turned out to depend more on the size of anions than on the nature of anions as long as the film was thin(a few hundred angstroms)<sup>15</sup>. The partial release of cations during oxidation of polypyrrole or other polymers(instead of anion uptake) will result in a reduced electrochemical equivalent weight of the cathode. This has the practical advantage of increasing the energy and power density for the polymer cathode energy storage system and the released cation sustains the conductivity of the electrolyte solution. However, further details of the oxidation/reduction process and the variation of the electrolyte concentration during the charge/discharge process will await future reports<sup>15,16</sup>.

## EXPERIMENTAL

### Solutions and Chemicals

All the chemicals used in this study were reagent grade. Acetonitrile(AN) (Burdick & Jackson) and doubly-distilled water were used as solvents. Solutions used for the preparation of polypyrrole films were AN containing  $0.2 \text{ mol dm}^{-3}$  pyrrole monomer and  $0.2 \text{ mol dm}^{-3}$  electrolytes of  $(\text{C}_4\text{H}_9)_4\text{NClO}_4$ ,  $(\text{C}_2\text{H}_5)_4\text{NBF}_4$ ,  $(\text{C}_2\text{H}_5)_4\text{NCH}_3\text{C}_6\text{H}_4\text{SO}_3$  (TEATOS). For electropolymerization in the presence of the polymer anions poly(vinylsulfonate) ( $\text{PVS}^-$ ) or poly(4-styrenesulfonate) ( $\text{PSS}^-$ ), aqueous solutions containing  $0.01 \text{ mol dm}^{-3}$  pyrrole monomer and  $0.01 \text{ mol dm}^{-3}$  electrolyte(KPVS or NaPSS) were used. The solutions were purged with  $\text{N}_2$  gas before polymer film formation on the quartz crystals.

### Film Preparation

A gold(ca.2000Å thick)-coated quartz crystal was employed as the substrate for polymer deposition. A large area of stainless steel was used as the counter electrode. The potentials were referred to a  $\text{Ag}/\text{Ag}^+$  ( $0.01 \text{ mol dm}^{-3} \text{ AgNO}_3/\text{Acetonitrile}$ ) or an SCE electrode for non-aqueous and aqueous solution systems respectively.

Polypyrrole films were grown on a quartz crystal where the potential was cycled between -1.5 and 0.8V(vs.  $\text{Ag}/\text{AgNO}_3(0.01 \text{ mol dm}^{-3})$ ) for non-aqueous and/or between -1.3 and 0.7V(vs. SCE) for aqueous electropolymerization systems. The non-aqueous systems were used for polypyrrole growth with  $\text{ClO}_4^-$ ,  $\text{BF}_4^-$ , and  $\text{TOS}^-$  anions, and the aqueous systems for  $\text{PVS}^-$  and  $\text{PSS}^-$  films. The chemical structure for anions used for electropolymerization are listed in Fig.1.

### QCM Measurements

A block diagram of the QCM apparatus interfaced with a potentiostat/galvanostat and a personal computer is shown in Fig.2. The working electrode was attached to both the oscillator and potentiostat and thereby to ground. As an alternative, a small capacitor (0.1  $\mu$ F) was inserted between the oscillator and potentiostat to avoid low frequency ground loops. We obtained identical results when the Princeton Applied Research 173 potentiostat was used in this mode, or without the capacitor, but in the former mode, the digital coulometer and current plot-in module was protected from damage. The current to the cell was always measured with a Keithley autoranging picoammeter in series with the counter electrode of the electrochemical cell. Shear mode 6MHz AT-cut quartz crystals (INFICON) were used for the investigation<sup>7</sup>. The crystals had vacuum deposited gold electrodes on both sides. The quartz plate was sealed to the cell with a silicone rubber sealant. The resonance frequency shift was measured with a Hewlett Packard frequency counter, and the data were stored in the computer. Experiments were carried out under nitrogen. The conducting polymer film in contact with the solution was the working electrode which was grounded through the potentiostat. As will be shown below, the mass of the deposited film was a linear function of the charge for all the films studied here, and thus may be taken as rigid. Since the film thickness of as-grown polypyrrole is small compared to the thickness of the crystal, and behaved in a rigid manner, the shear wave is not significantly damped<sup>1</sup>. With an increase of polymer film mass, the resonant frequency obeys the following equation<sup>17</sup>:

$$\Delta f = - \frac{2f_0^2}{\sqrt{\rho_{\Omega}\mu_{\Omega}}} \frac{\Delta m}{A} \quad [1]$$

For the quartz crystal used here(6 MHz Inficon), the relationship between frequency shift( $\Delta f$  [Hz]) and mass change( $\Delta m$  [ng]) is simply expressed as follows;

$$\Delta f = -0.0825 \frac{\Delta m}{A} \quad [2]$$

where  $A$  is the electrochemically and piezoelectrically active surface area of the quartz crystals ( $0.33 \text{ cm}^2$ ).

The mass change and the cyclic voltammetric measurement were performed at the same time during electropolymerization and the redox cycling (up to ca. 25% of the doping level) at a sufficiently slow sweep rate of  $10 \text{ mV s}^{-1}$  so that the electrode system was completely under thermodynamic control and should be considered free from kinetic or transport effects. The cyclic voltammograms and the maximum change in mass did not change appreciably when the cycling was performed at slower sweep rate.

## RESULTS AND DISCUSSION

Figure 3 shows a typical cyclic voltammogram and mass change for the electropolymerization of pyrrole in the presence of a small anion, viz.,  $\text{BF}_4^-$  in the solution containing both pyrrole monomer and electrolyte. Polypyrrole begins to grow above 0.3 V and the current for growth increases almost linearly with an increase in potential and time. Subsequent cycling at potentials between -0.5 and 0.0 V shows a set of peaks which are ascribed to the charge injection/release of the grown polypyrrole film. During the cyclic voltammetry, the mass of the film changes with an increase in potential. At potentials beyond about 0.3 V, polypyrrole continued to grow almost at a constant rate. During the reduction process subsequent to the formation of the polymer film, the mass did not change significantly. This means that the mass change due to the redox process (insertion/extraction of ions) is relatively small compared to that associated with electropolymerization. The variation of the  $Q$  and  $\Delta m$  values appear to be identical, suggesting that the charge consumed leads to the mass change on quartz crystals. The fact that the charge

decrease (between 0.0 to -1.5 V) corresponds to a decrease in mass, indicates the film releases anions during the reduction process. Electropolymerization and redox behavior of pyrrole with  $\text{ClO}_4^-$  exhibits the same trend in the relationship between charge and  $\Delta m$  as seen with  $\text{BF}_4^-$  (see Fig.4).

In order to confirm the rigidity of the film or applicability of Eq.[1] to the polypyrrole films, the mass change,  $\Delta m$  was plotted against charge,  $Q$  which is consumed during the electropolymerization. The same data in Fig.3 was used to plot this and is shown in Fig.4. There seem to be two linear regions which corresponds to the two different polymer growth rate. The first ( $Q < \text{ca. } 6500 \text{ mC}$ ) would be the nucleation region, and the latter ( $Q > 7000 \text{ mC}$ ) would correspond to the polymer film growth. Linear relationship between the charge and the mass change is observed for almost the entire range of polymer growth. Since the mass of deposited polymer is linearly correlated with the amount of charge passed during electropolymerization<sup>19</sup>, one can treat the grown film as rigid and free from viscoelastic effects. Also, the same confirmation of rigidity was made for the polypyrrole films grown with other anions, and they all show the similar behavior (linearity between  $Q$  and  $\Delta m$ ) for the entire region of charge, thickness or potential studied in the present investigation.

The same experiment as in Fig.3 was performed using a medium sized tosylate ( $\text{TOS}^-$ ) anion. Figure 5 shows a typical cyclic voltammogram and the mass change during electropolymerization of pyrrole (beyond ca. 0.4V) and subsequent reduction and reoxidation (-1.1 to -0.2V). After the potential was scanned from 0.3V, the polypyrrole grew on the quartz crystal until the potential scan was reversed and ramped from 0.8V to 0.4V. Around -0.75V, there was a cathodic peak due to the reduction process. At the same time, the mass of the film increased, indicating that cations ( $\text{TEA}^+ = (\text{C}_2\text{H}_5)_4\text{N}^+$ ) were incorporated into the film in order to maintain charge neutrality. After the peak, the mass decreased indicating anion movement out of the film. After scanning back from -1.5 to

0.5V, there was an decrease in mass of lower magnitude than that occurring during reduction, which suggests that both cations and anions were removed during the oxidation process.

In Fig.6, the current, charge and mass change from the same data in Fig.5 are replotted against time. When one looks at the oxidation and/or reduction peaks, there is a reverse trend for the relationship between charge and mass change compared to the behavior with  $\text{BF}_4^-$  and  $\text{ClO}_4^-$ . This may suggest that anions as well as cations were involved in the redox process. Also, there is a hysteresis behavior at -0.2V for both charge and mass change. This indicates that the coulombic efficiency was not 100% for the very first cycle after the electropolymerization of the film with  $\text{TOS}^-$  anions. However, after cycling several times the curve returns to the initial frequency. The coulombic efficiency was almost completely 100% for  $\text{BF}_4^-$  when one compares the curves at the same potential. This indicates that small ions with higher nucleophilic character will have higher apparent coulombic efficiency for initial cycling.

Cycled potential electropolymerization was also performed with large polymeric anions like  $\text{PSS}^-$  or  $\text{PVS}^-$ . Figure 7 shows the time vs.  $Q$ ,  $\Delta m$  plots for electropolymerization of pyrrole with  $\text{PSS}^-$  anions. Unlike the polymer growth with smaller anions, eg.,  $\text{BF}_4^-$  and  $\text{ClO}_4^-$ , the mass increased during the film reduction process. This suggests that the film incorporated cations in the reduction process instead of releasing anions because the large anions could not be untangled from the polypyrrole matrix<sup>18</sup>. In the case of electropolymerization with  $\text{PVS}^-$  anions, a similar behavior was observed(see Fig.8).

In order to look more carefully at the stoichiometry of the redox process subsequent to the electropolymerization, the mass change obtained by QCM measurement was compared to that calculated from the charge, assuming specific ions to be involved in the process. In Fig.9, the analysis was made for polypyrrole/ $\text{BF}_4^-$  film undergoing the



reduction reaction.  $\Delta m(\text{QCM})$  and  $\Delta m(\text{Q})$  represent the mass changes obtained from the QCM measurement and the charge, respectively. In this case, the mass change ( $\Delta m(\text{Q})$ ) was obtained assuming that only anions ( $\text{BF}_4^-$ ) were extracted during the reduction process after electropolymerization. Initially the values of  $\Delta m(\text{QCM})$  and  $\Delta m(\text{Q})$  agree well, indicating that only anions were removed in the reduction reaction. However, at high stages of reduction (or discharge) (below  $-350 \mu\text{C}$ ), the two values begin to deviate<sup>15b</sup>. This suggests that cations are inserted to compensate the negative charges of anions which are trapped deeply inside the bulk of polymer, and are not completely recovered at high level of reduction. This explanation would be possible provided that the mass change due to the solvent motion can be assumed to be negligible compared to the ion insertions or extractions. Considering that the polypyrrole films usually shrink by releasing solvents or electrolytes from the film when they are reduced or undoped, ascribing the mass gain in this potential region to solvent ingress does not seem well founded without further work. If the charge compensation by the cation is assumed, the ion insertion behavior can be discussed generally in conjunction with that observed for polypyrrole/ $\text{TOS}^-$  film which shows cation insertion at relatively shallow level of reduction compared to  $\text{BF}_4^-$ .

The analysis was made also for  $\text{TOS}^-$  which is a medium sized anion investigated in the present paper. Figure 10(upper) shows the results for a PPy/ $\text{TOS}^-$  film. The  $\Delta m(\text{QCM})$  curve lies between the  $\Delta m(\text{Q})$  values assuming exclusively anion ( $\text{TOS}^-$ ) or exclusively cation ( $\text{TEA}^+$ ) motion during the reduction process. There is a clear indication here that both anions and cations move during the reduction process, at proportions which depend on the charge. The proportion of cation to anion ( $\frac{C}{C+A}$ ) in the PPy/ $\text{TOS}^-$  film was calculated by  $\Delta m(\text{Q})$  to  $\Delta m(\text{QCM})$  at each data point. In Fig.9(lower), the  $\frac{C}{C+A}$  variation is plotted against the charge during the reduction process. At low levels of reduction (less than  $-100 \mu\text{C}$ ), mostly anion motion seems to be involved in the charge-compensation process, and the cation contribution is below 70%. As the film becomes more

reduced (more than  $-200 \mu\text{C}$ ), the contribution of cation motion becomes more significant. Finally, the ratio levels off at 100%, indicating that the charge is compensated by only cations. This fact may be associated with the relative mobility of anions ( $\text{TOS}^-$ ) and cations ( $\text{TEA}^+$ ) in the film which would be expected to be strongly influenced by the size of the ions. The fact may also be caused by thermodynamic constraints on ionic composition of the  $\text{PPy}/\text{TOS}^-$  film. The reason for the behavior could involve ion-ion and ion-solvent (*solvation effects*) interactions inside the film, but it is not clear from the present data.

Figure 11 shows the same analysis for  $\text{PPy}/\text{PVS}^-$  and  $\text{PPy}/\text{PSS}^-$  films. For the  $\text{PVS}^-$  case, the  $\Delta m(\text{QCM})$  value shows a good agreement with the  $\Delta m(\text{Q})$  curve where 1 Faraday of charge is compensated with one mole of cation ( $\text{K}^+$ ) and at the same time two moles of solvent ( $\text{H}_2\text{O}$ ) are extracted from the film during the reduction process. For the  $\text{PSS}^-$  case, the two curves show agreement when the insertion of one cation ( $\text{Na}^+$ ) and the extraction of one solvent molecule ( $\text{H}_2\text{O}$ ) are assumed. There is an indication that less than 100% of cation charge compensation occurs but other species in the solvent (e.g.,  $\text{OH}^-$ ,  $\text{H}_2\text{O}$  or  $\text{H}_3\text{O}^+$ ) are involved in the process of reduction in  $\text{PPy}/\text{polymer anion composite}$  films. The possible explanation could be the following: during electropolymerization (oxidation) of pyrrole, both polymeric anion ( $\text{SO}_3^-$  sites) and species from the solvent act as dopants for the compensation of the positive charge created by the radical cations. The  $\text{SO}_3^-$  sites in the polymer anion can not compensate the positive charge in the polymer due to steric hindrance and mismatch of the distance between active sites. The positive sites may also be solvated with more than two molecules of  $\text{H}_2\text{O}$ , and compensation by  $\text{OH}^-$  ions may also be important effects during electropolymerization. During the reduction process of the film, excess solvent might also be removed at the same time that cation moves in. The complex processes in the composite films may include morphological or volumetric changes as well, but further analysis must await more detailed studies.

## CONCLUSIONS

Ion(anion and/or cation) motion during redox processes seems to depend strongly on the size of anions. Figure 12 summarizes briefly the ion motion during oxidation/reduction of polypyrrole films. The polypyrrole film prepared with small anions like  $\text{ClO}_4^-$  and  $\text{BF}_4^-$  showed exclusively anion doping during the oxidation process which means that only anions act in the role of charge compensation of the oxidized sites in the polymer. The films formed with large polymeric anions like  $\text{PSS}^-$  and  $\text{PVS}^-$  showed in turn mostly cation and solvent( $\text{OH}^-$  in aqueous solution) charge compensation during the oxidation process. The films prepared with medium size anions like  $\text{TOS}^-$ , showed a somewhat intermediate behavior, i.e., both anion and cation motions were observed during the oxidation and reduction process.

On the basis of the above concept, the electrochemical equivalent for Anode/Electrolyte/Polymer cathode cell systems are compared in Fig.13. For usual polymer cathode cell systems(small anions( $\text{ClO}_4^-$ ,  $\text{BF}_4^-$ ), doped polypyrroles), one must consider that the charge/discharge process requires an equivalent amount of electrolyte in charge-based calculations. In this case, most of the cell weight is composed of the weight of the electrolyte solution. Even if we use a very concentrated solution, the electrolyte accounts for more than 50% of the weight and volume(e.g.,  $4 \text{ mol dm}^{-3}$   $\text{LiClO}_4$  in propylene carbonate), and results in a lower energy density( $150 \text{ Wh kg}^{-1}$  of theoretical specific energy per cell without hardware<sup>16</sup>) compared to cation insertion compounds like  $\text{V}_2\text{O}_5$  or  $\text{TiS}_2$ . However, using relatively large anions as dopants as in the present study, one needs less electrolyte to sustain charge/discharge reactions. For the polypyrrole films with incorporated polymeric anions like  $\text{PPy/PSS}^-$  and  $\text{PPy/PVS}^-$ , it appears that mostly cation motion is observed during the oxidation/reduction process and only a small amount of electrolyte is required, and the cells have a higher energy density.

#### ACKNOWLEDGEMENT

The authors wish to acknowledge the financial support of the Defense Advanced Research Projects Agency and the Office of Naval Research(DARPA/ONR).

#### References

1. M.R.Deakin and O.Melroy, *J. Electroanal. Chem.*, **219**, 321 (1988).
2. M.Benje, M.Eier, U.Pittermann and K.G.Weil, *Ber. Buns. Phys. Chem.*, **90**, 435 (1986).
3. J.H. Kaufman, K.K. Kanazawa and G.B. Street, *Phys. Rev. Lett.*, **53**, 2461 (1984).
4. D. Orata and D.A. Buttry, *J. Am. Chem. Soc.*, **109**, 3574 (1987).
5. (a) P.T. Varineau and D.A. Buttry, *J. Phys. Chem.*, **91**, 1292 (1987);  
(b) M.D. Ward, *J. Phys. Chem.*, **92**, 2049 (1988).
6. C.J.Chandler, J-B Ju, R.Atanasoski and W.H.Smyrl, Corrosion '89, paper p.37, NACE (New Orleans), April, (1989).
7. S. W. Feldberg, *J. Am. Chem. Soc.*, **106**, 4671 (1984).
8. B. J. Feldman, P. Burgermayer and R. W. Murray, *J. Am. Chem. Soc.*, **107**, 872 (1985).
9. (a) J. Tanguy, N. Mermilloid and M. Hoclet, *Synth. Met.*, **18**, 7 (1987).  
(b) J. Tanguy and N. Mermilloid, *Synth. Met.*, **21**, 129 (1987).  
(b) J. Tanguy, N. Mermilloid and M. Hoclet, *J. Electrochem. Soc.*, **134**, 795 (1987).
10. (a) C. Ho, I. D. Raistrick and R. A. Huggins, *J. Electrochem. Soc.*, **127**, 343 (1980);  
(b) T. B. Hunter, P. S. Tyler, W. H. Smyrl and H. S. White, *J. Electrochem. Soc.*, **134**, 2198 (1987);

- (c) K. Naoi, K. Ueyama, T. Osaka and W. H. Smyrl, *J. Electrochem. Soc.*, **137**(2), in press.
- (d) T. Osaka and K. Naoi, *Bull. Chem. Soc. Jpn.*, **55**, 36 (1982).
11. M. Lien and W. H. Smyrl, Proc. of 174th ECS Meeting(Trans. Tech. in Corr. Sci & Eng.), p.286 (1988).
12. T. Osaka, S. Ogano, K. Naoi, and N. Oyama, *J. Electrochem. Soc.*, **136**, 306 (1989).
13. (a) K. Naoi and T. Osaka, *J. Electrochem. Soc.*, **134**, 2479 (1988);  
(b) K. Naoi, B. B. Owens, M. Meda and T. Osaka, Proc. of 174th ECS Meeting, Chicago (1988), **88-6**, 770 (1988).
14. W. H. Smyrl, R. T. Atanasoski, L. Atanasoski, L. Hartshorn, M. Lien, K. Nygren and E. A. Fletcher, *J. Electroanal. Chem.*, **264**, 301 (1989).
15. (a) K. Naoi, M. M. Lien and W. H. Smyrl, *J. Electroanal. Chem.*, in press;  
(b) K. Naoi and W. H. Smyrl, *J. Electrochem. Soc.*, submitted.
16. K. Naoi, B. B. Owens and W. H. Smyrl, *Proc. Symp. Li. Bat., 176th ECS Meeting, Hollywood (Oct., 1989)*, to be published.
17. G. Sauerbrey, *Z. Phys.*, **155**, 206 (1959).
18. (a) T. Shimidzu, A. Ohtani, T. Iyoda and K. Honda, *J.C.S Chem. Commun.*, **1986**, 1415.  
(b) T. Iyoda, A. Ohtani, T. Shimidzu and K. Honda, *Chem. Let.*, **1986**, 687.  
(b) T. Shimidzu, A. Ohtani, T. Iyoda and K. Honda, *J. Electroanal. Chem.*, **22** 23 (1987).
19. C. K. Baker and J. R. Reynolds, *J. Electroanal. Chem.*, **251**, 307 (1988).

## Figure Captions

- Fig.1 Schematics of anions used during electropolymerization of polypyrrole.
- Fig.2 Schematic diagram of QCM apparatus interfaced with electrochemical potentiostat/galvanostat and personal computer <sup>6</sup>.
- Fig.3 Typical cyclic voltammogram and mass change for polypyrrole growth and redox process under cycled potential ( $v=10 \text{ mV s}^{-1}$ ) in ( $0.2 \text{ mol dm}^{-3} \text{ TBABF}_4 + 0.2 \text{ mol dm}^{-3} \text{ pyrrole}$ ) in acetonitrile.
- Fig.4 Plots of mass change ( $\Delta m$ ) vs. charge ( $Q$ ) during polypyrrole growth in ( $0.2 \text{ mol dm}^{-3} \text{ TBABF}_4 + 0.2 \text{ mol dm}^{-3} \text{ pyrrole}$ ) in acetonitrile.
- Fig.5 Typical cyclic voltammogram and mass change for polypyrrole growth and redox process under cycled potential ( $v=10 \text{ mV s}^{-1}$ ) in ( $0.2 \text{ mol dm}^{-3} \text{ TBAClO}_4 + 0.2 \text{ mol dm}^{-3} \text{ pyrrole}$ ) in acetonitrile.
- Fig.6 Typical cyclic voltammogram and mass change ( $\Delta m$ ) for polypyrrole growth and redox process under cycled potential ( $v=10 \text{ mV s}^{-1}$ ) in ( $0.2 \text{ mol dm}^{-3} \text{ TEATOS} + 0.2 \text{ mol dm}^{-3} \text{ pyrrole}$ ) in acetonitrile.
- Fig.7 Time vs. charge ( $Q$ ), mass change ( $\Delta m$ ), and current curves for the same data in Fig.5.
- Fig.8 Time vs. charge ( $Q$ ), mass change ( $\Delta m$ ), and current curves for the electrochemical growth and redox process of the polypyrrole film grown in the presence of NaPSS. The data were shown in the region of redox cycling where the potential region is between  $-1.5$  and  $0.2 \text{ V}$ .
- Fig.9 Time vs. charge ( $Q$ ) and mass change ( $\Delta m$ ) for the growth and redox cycling of the polypyrrole film grown in the presence of KPVS.
- Fig.10 Charge vs. mass change ( $\Delta m(\text{QCM})$  and  $\Delta m(Q)$ ) for  $\text{PPy/BF}_4^-$  film.
- Fig.11 Upper: Charge vs. mass change ( $\Delta m(\text{QCM})$  and  $\Delta m(Q)$ ) for  $\text{PPy/TOS}^-$  film

which is grown in TEATOS solutions;

Lower: Charge vs. ratio of cation insertion during the reduction process.

Fig.12 Upper: Charge vs. mass change( $\Delta m(\text{QCM})$  and  $\Delta m(\text{Q})$ ) for PPy/PVS<sup>-</sup> film;

Lower: Charge vs. mass change( $\Delta m(\text{QCM})$  and  $\Delta m(\text{Q})$ ) for PPy/PSS<sup>-</sup> film.

Fig.13 Schematic models for ion insertions during redox process of polypyrrole.

Fig.14 Schematic of the equivalent cell weight for three different polymer cathode cell systems.

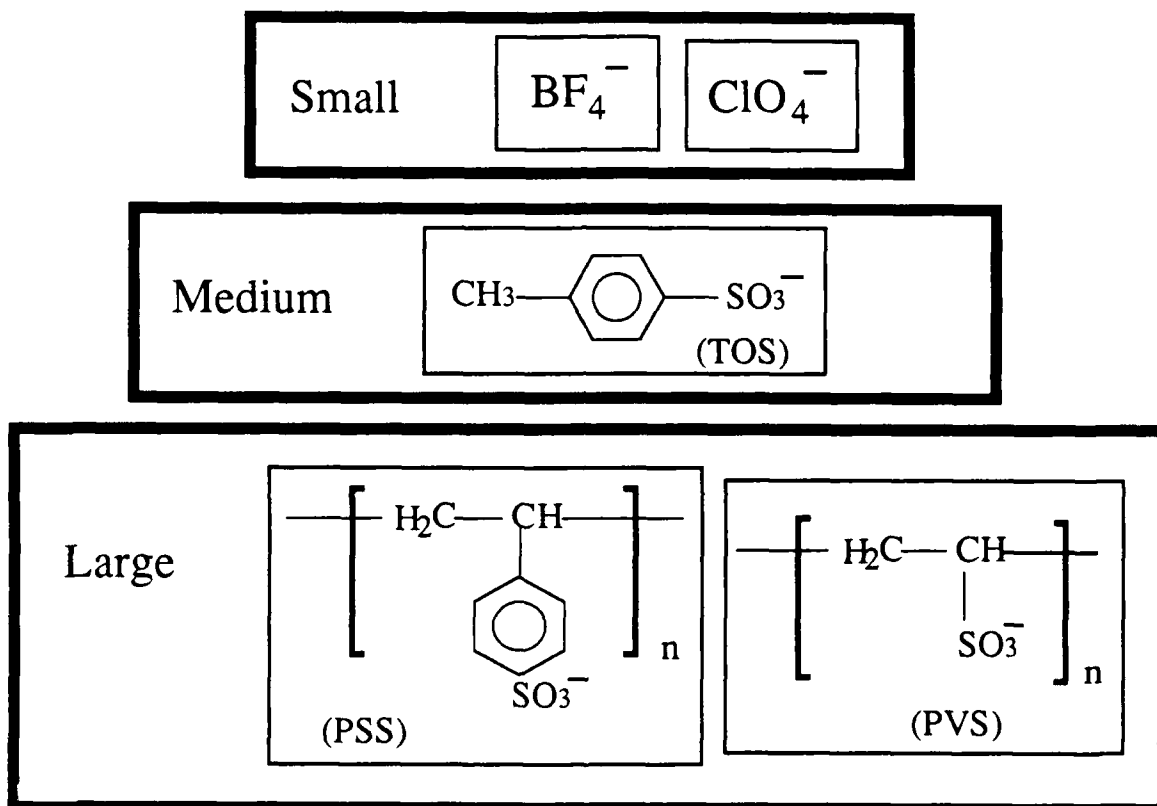
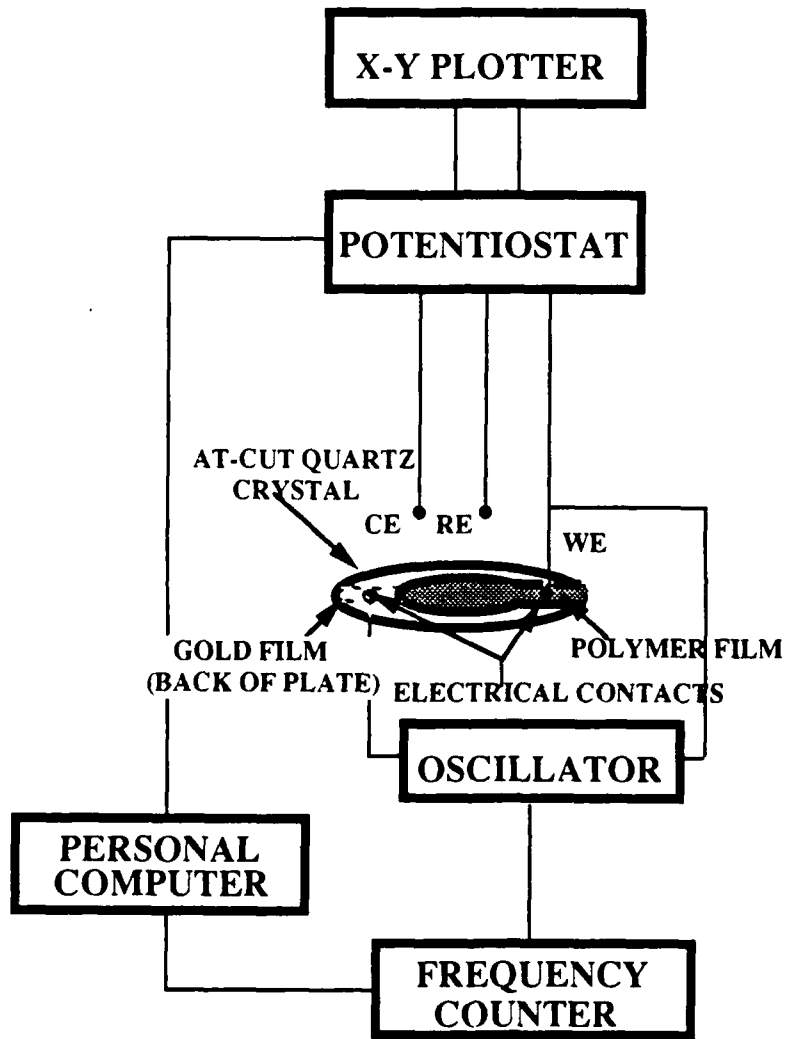


Fig.1





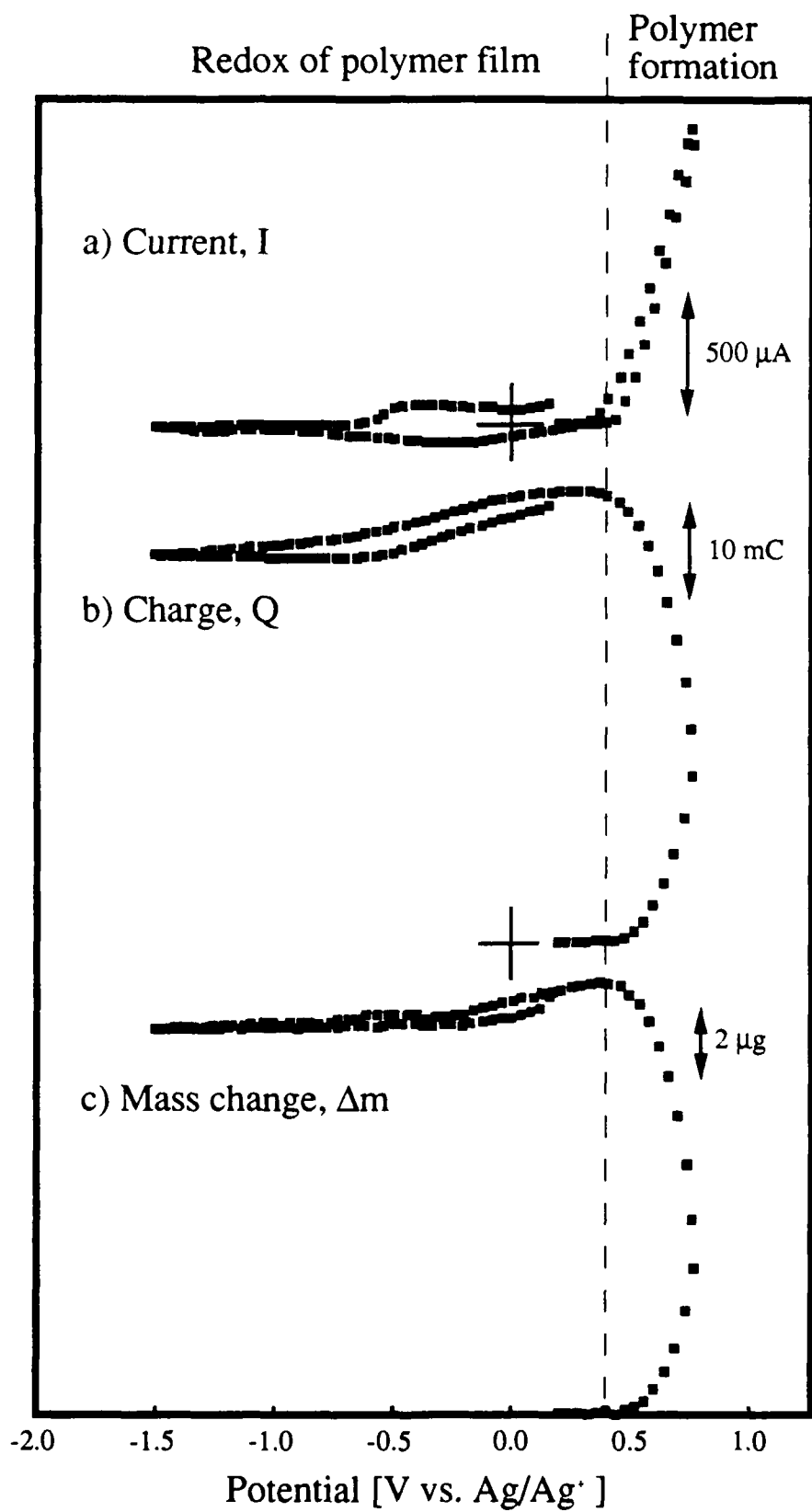


Fig.3

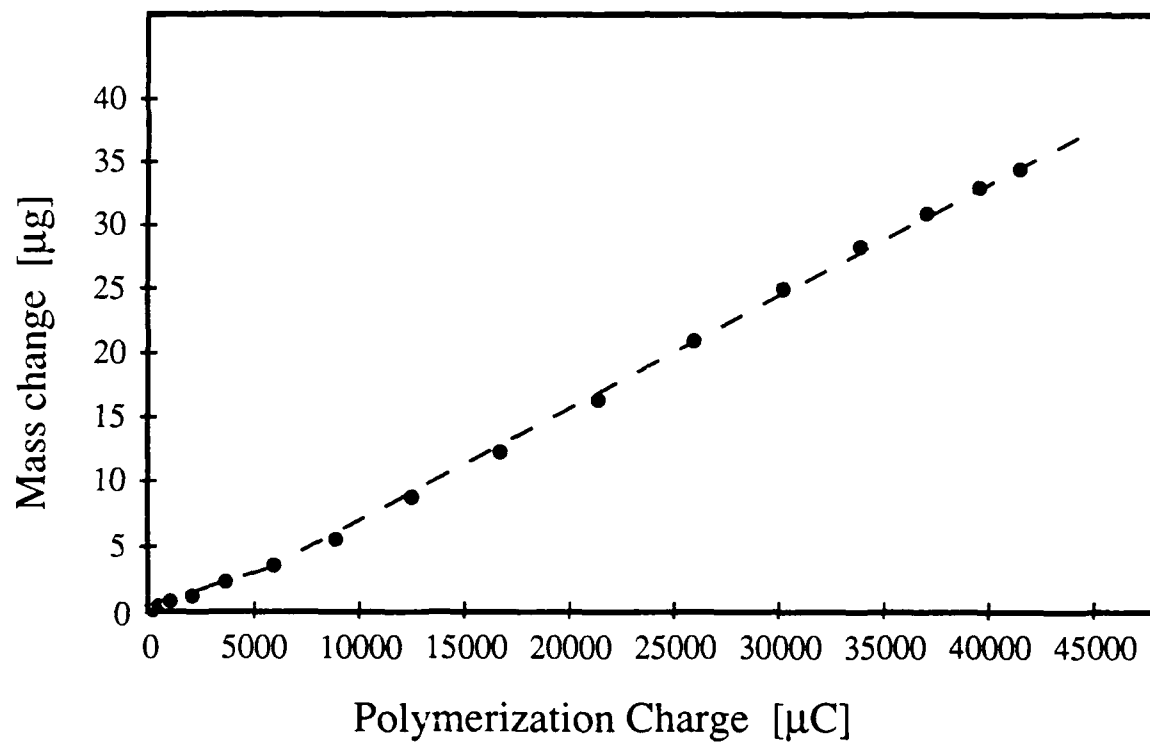


Fig.4 -Added

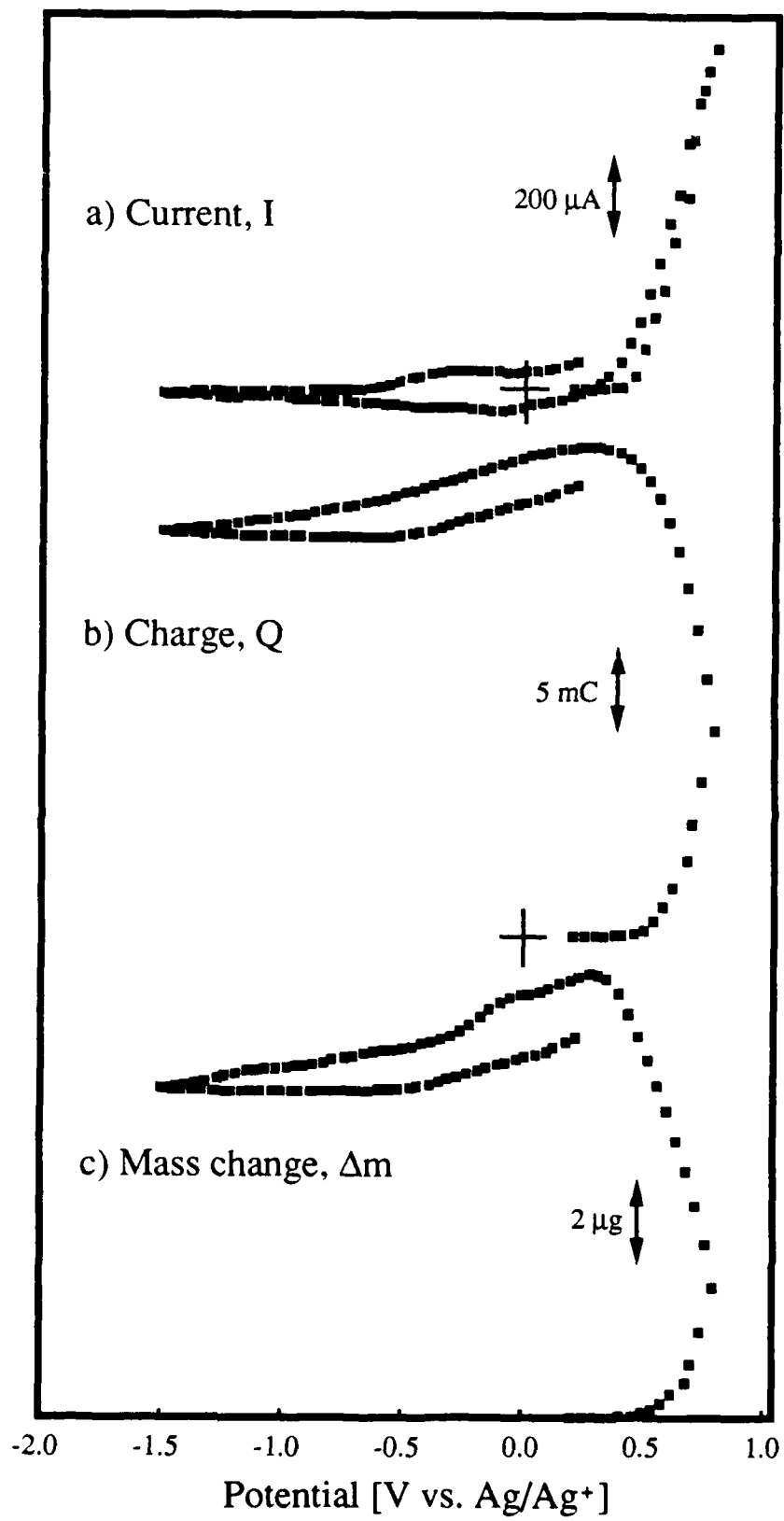


Fig.5

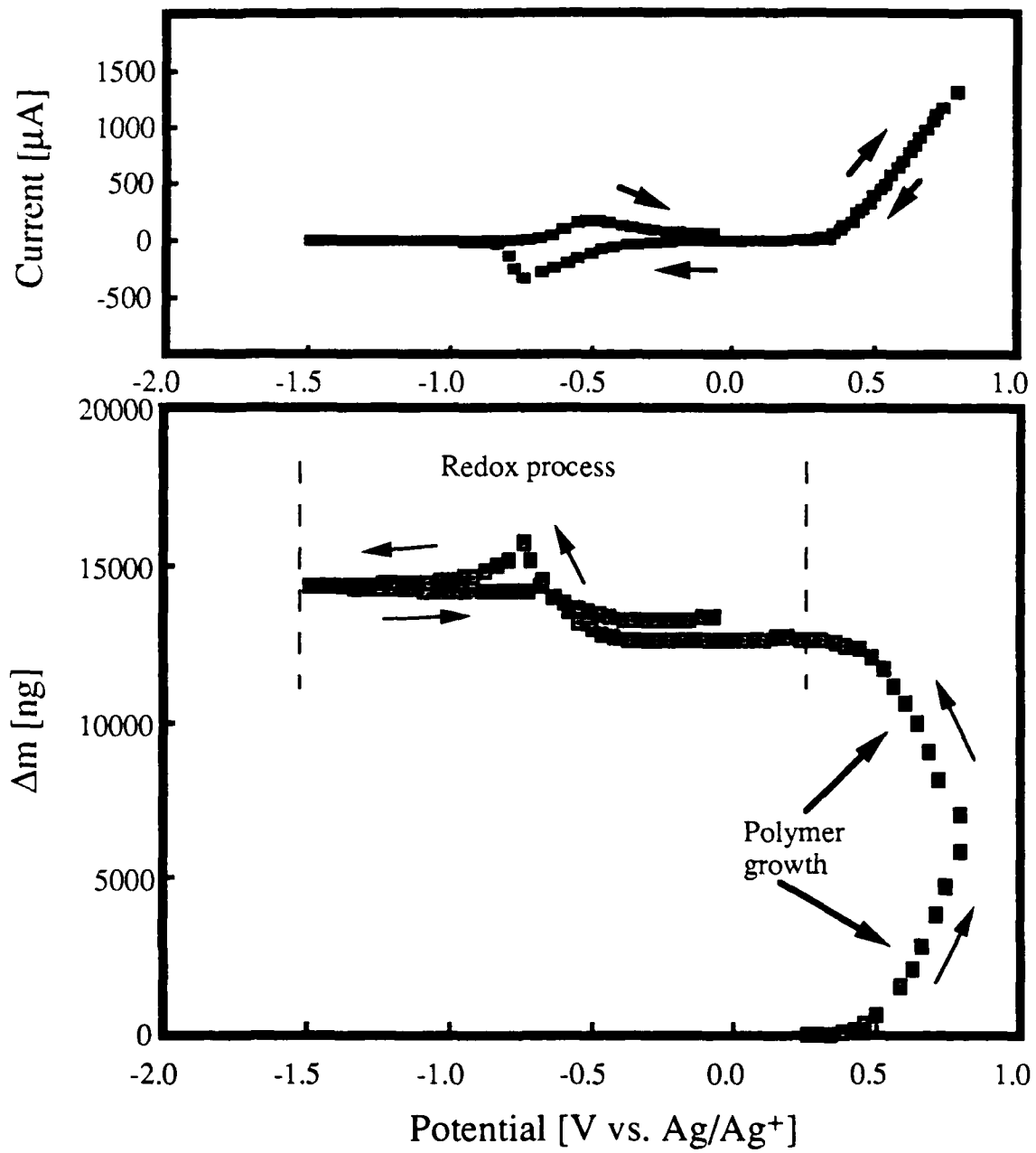


Fig.6

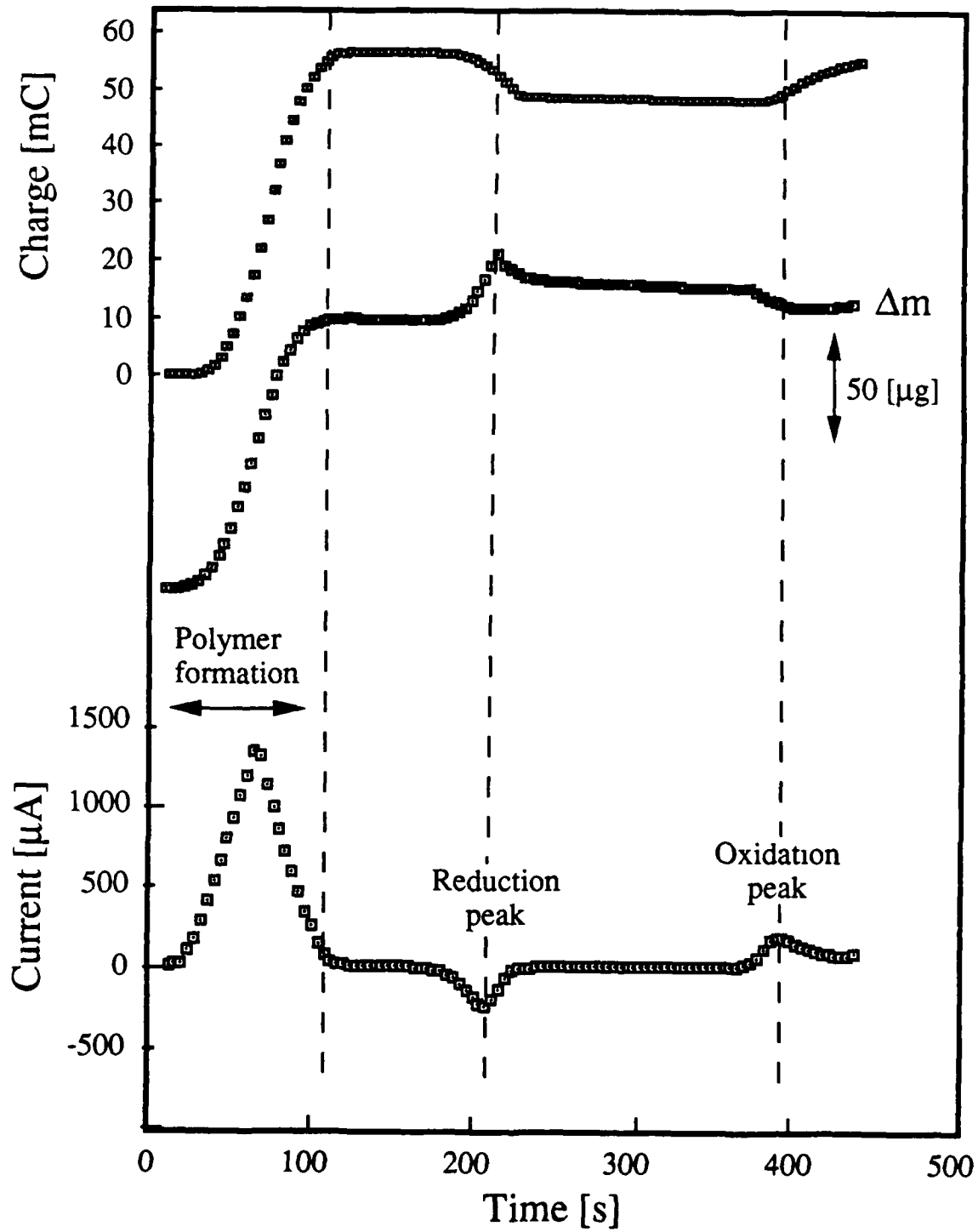


Fig.7

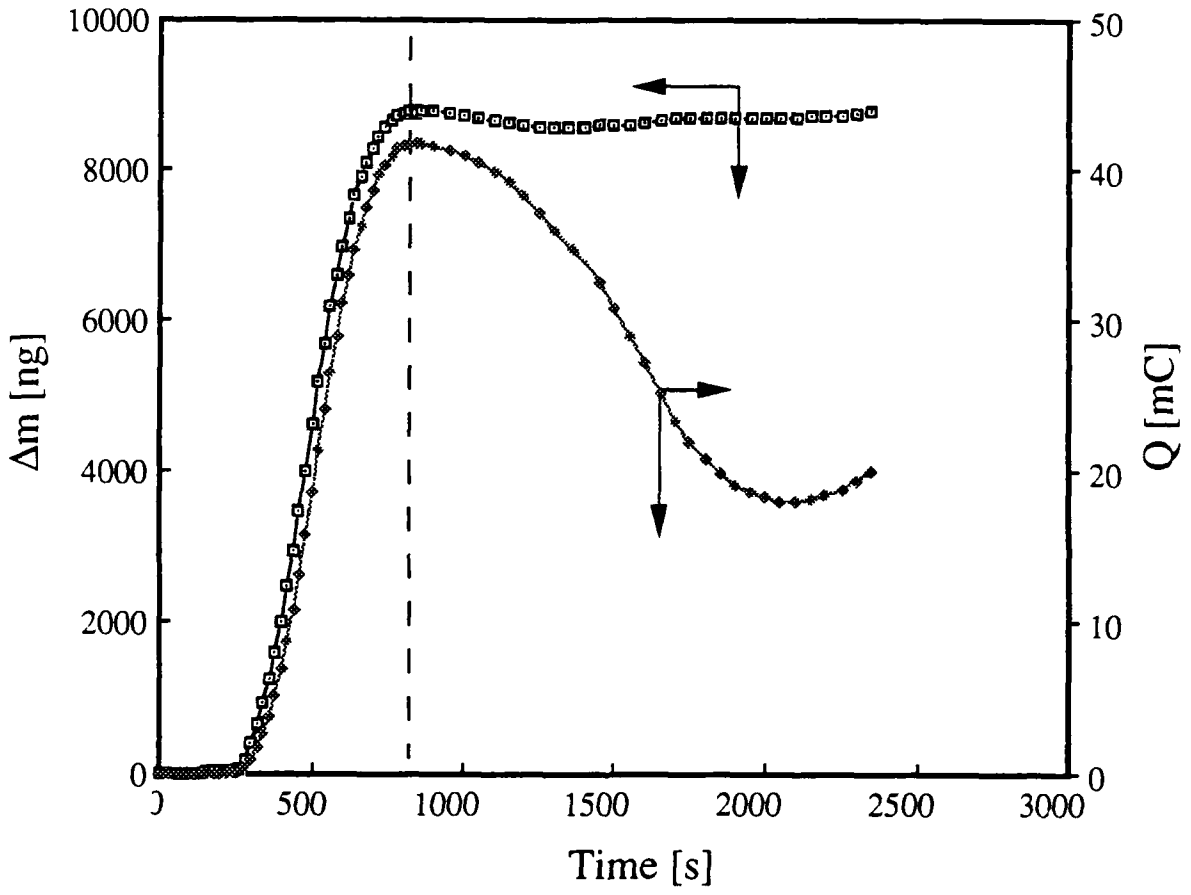


Fig.8

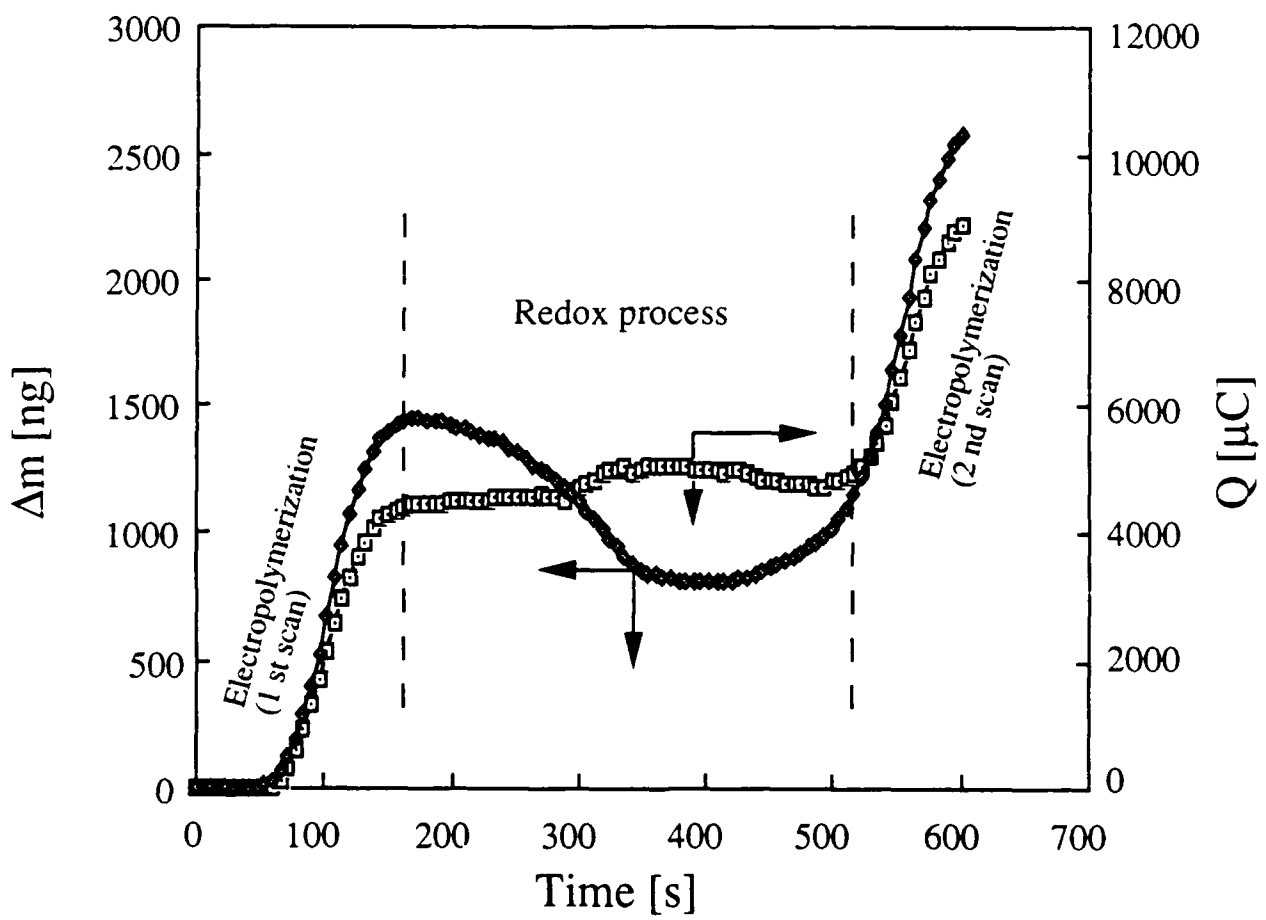


Fig.9



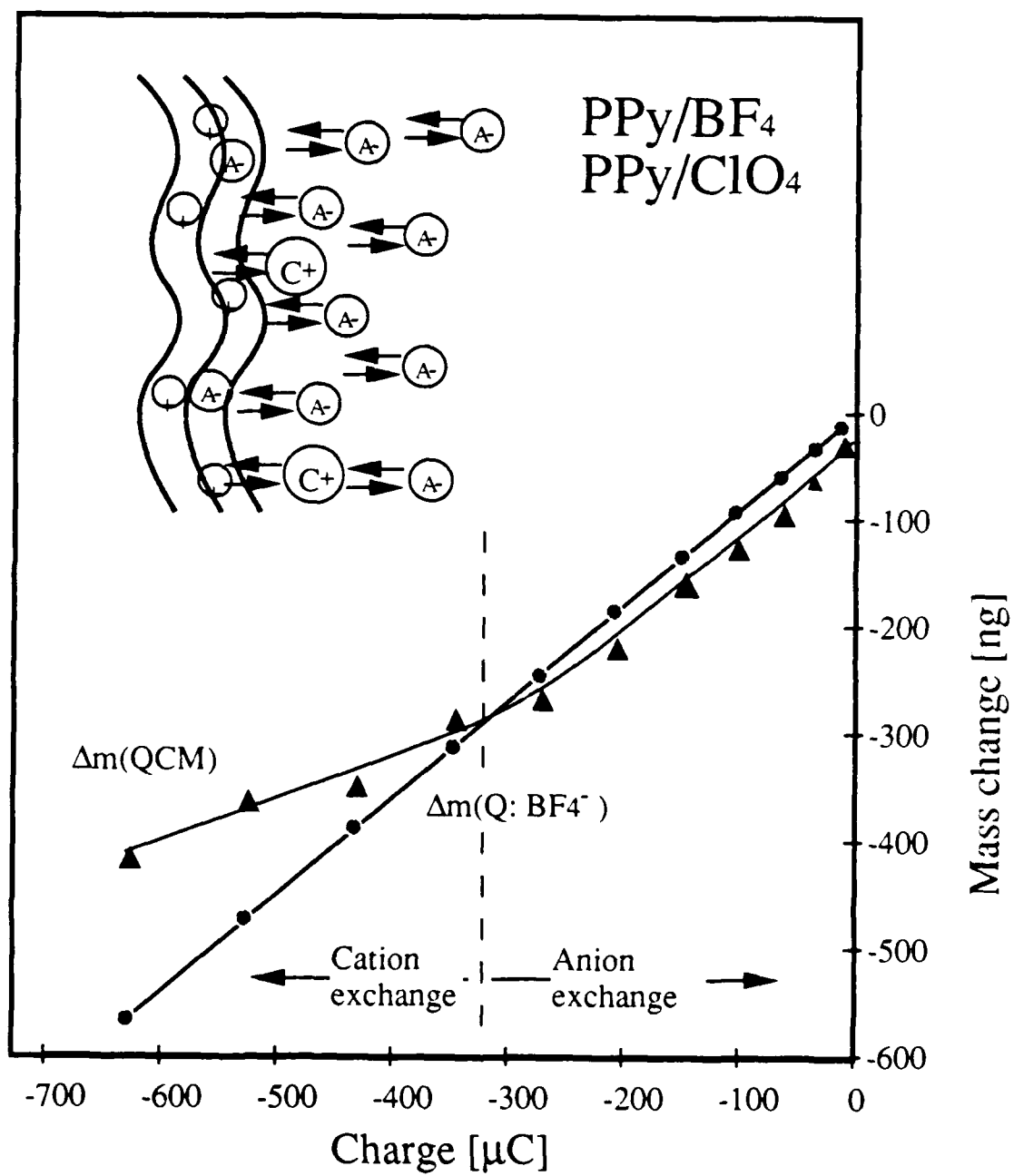


Fig.10

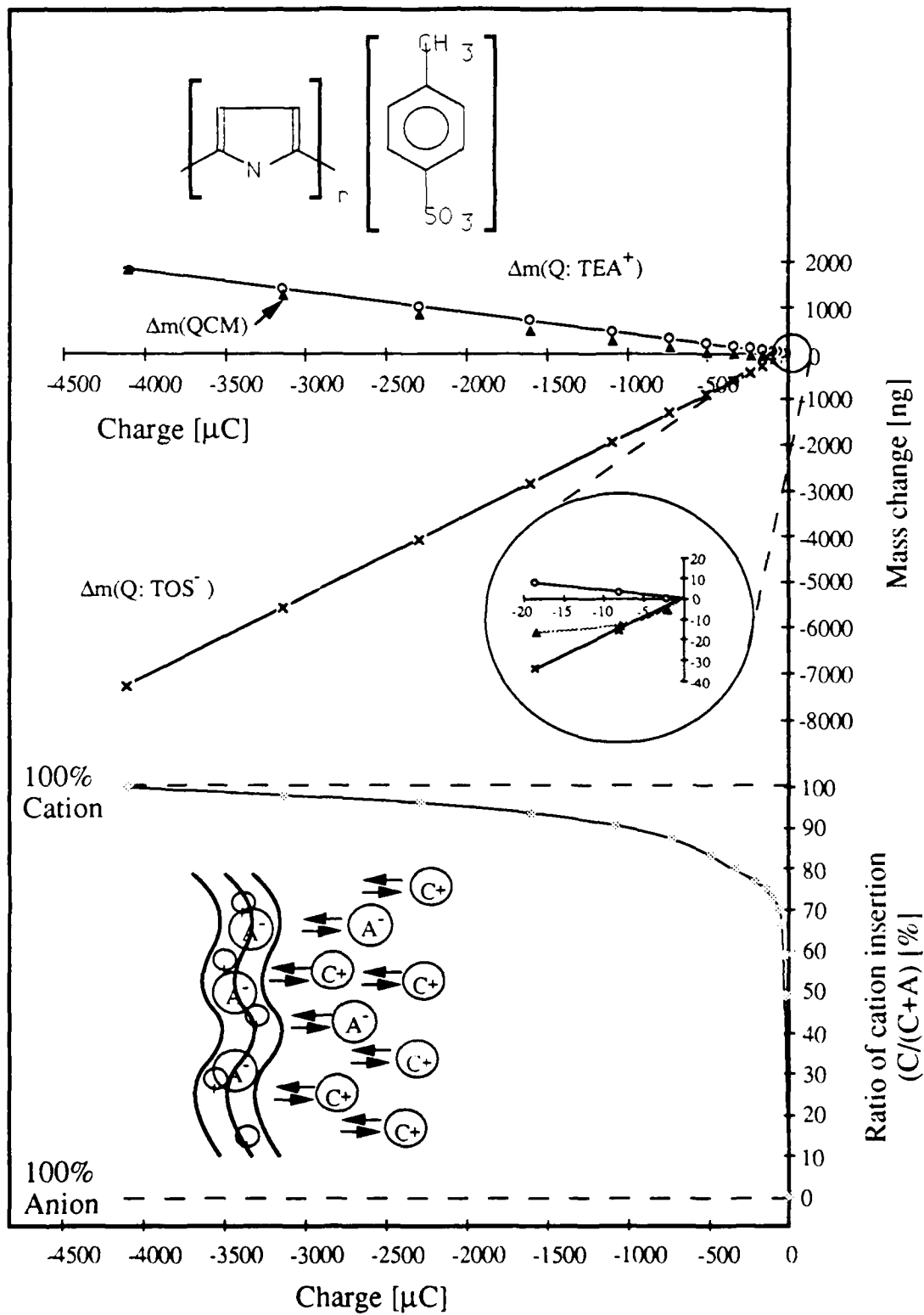


Fig. 11

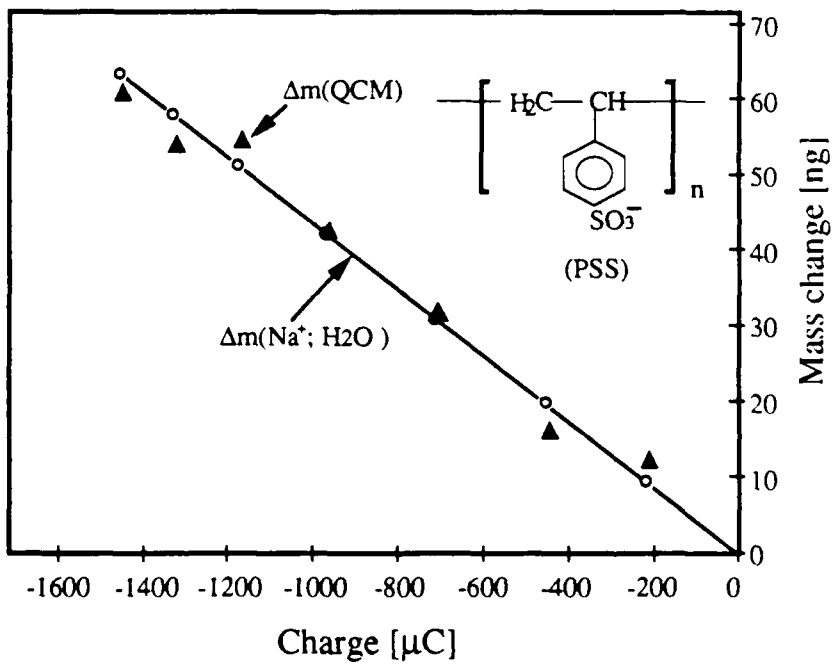
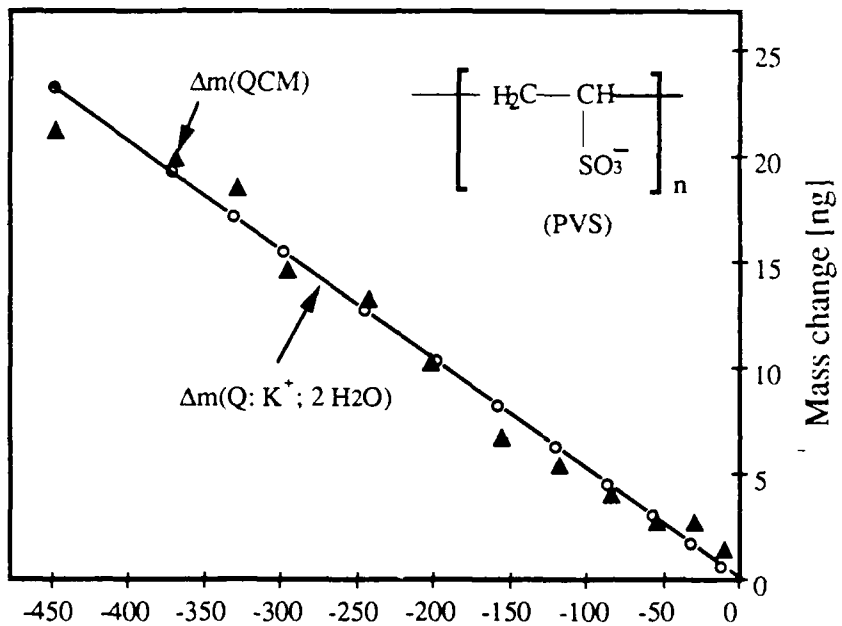
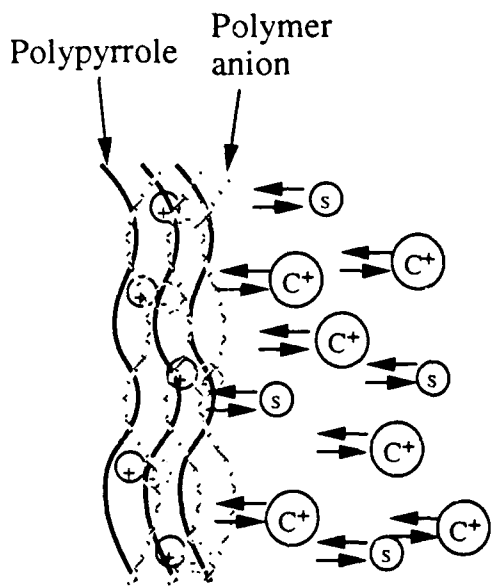
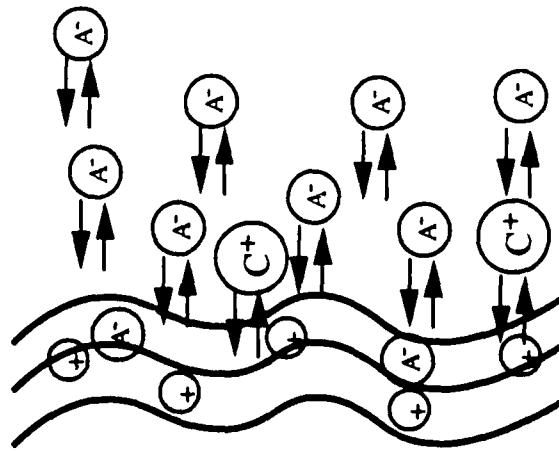
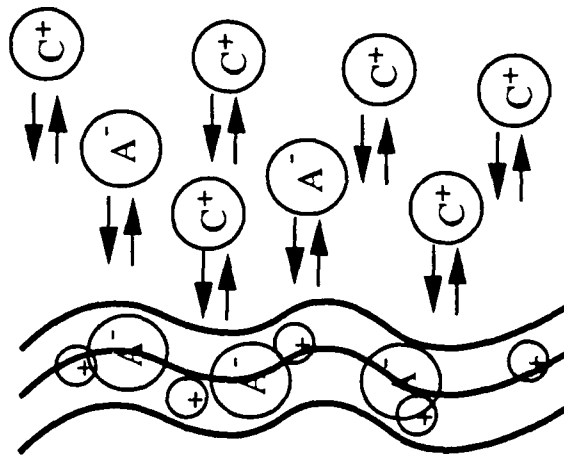


Fig.12

a) PPy/BF<sub>4</sub>, PPy/ClO<sub>4</sub>



b) PPy/TOS



c) PPy/PSS, PPy/PVS

